Haptic recognition of dystonia and spasticity in simulated multi-joint hypertonia

D. Piovesan[†]*, *IEEE Member*, A. Melendez-Calderon[†], *IEEE Member*, F.A. Mussa-Ivaldi

***Abstract*— This paper investigates the capability of naïve individuals to recognize dystonic- or spastic- like conditions through physical manipulation of a virtual arm. Subjects physically interact with a two-joint, six-muscle hypertonic arm model, rendered on a two degrees-of-freedom robotic manipulandum. This paradigm aims to identify the limitation of manual manipulation during diagnosis of hypertonia. Our results indicate that there are difficulties to discriminate between the two conditions at low to medium level of severity. We found that the sample entropy of the executed motion and the force experienced during physical manipulation, tended to be higher during incorrectly identified trials than in those correctly assessed.**

***Index Terms*—hypertonia, spasticity, rigidity, dystonia, assessment, haptic discrimination**

I. Introduction

HYPERTONIA is a frequent condition that contribute to reduced voluntary motor performance or involuntary muscle in neurological disease such as cerebral palsy, Parkinson's disease or after stroke [1, 2]. Hypertonia is characterized by a concurrent manifestation of symptoms that can include active contraction of the muscle at rest, hyperexcitability of motoneurons and excessive co-activation , muscle contracture and other impairments that induce an abnormal increase in resistance to externally imposed movement [3]. Depending on the pathophysiology, hypertonia can be referred as spastic hypertonia, rigidity, dystonic hypertonia, among others. Accurately diagnosing of the intrinsic characteristics of hypertonia is vital to determine appropriate interventions or treatment outcomes [3]. An erroneous clinical decision can lead to an increased treatment time, rise in overall costs, or even be detrimental for the overall condition. Therefore, the simultaneous manifestation of such conditions presents unique challenges for diagnosis.

To make an overall assessment of hypertonia, therapists physically manipulate the patients' limb so that each joint is tested individually; these movements are then rated by the therapists using current clinical scales (e.g. modified Ashworth scale, Tardieu scale, Hypertonia Assessment Tool) [4-7]. However, it would be useful to extend the assessment of hypertonia to multiple degrees of freedom at the same time, so to capture alteration of inter-muscular (heteronymous) reflexes [8] or abnormal multi-joint couplings [9, 10].

The quantitative measure of limb mechanics is crucial for an accurate diagnosis. Several system-identification methods have been proposed encompassing non-parametric [11-14] and parametric modeling [15, 16]. Such assessments ought to be preferred for accurate diagnoses but require sophisticated set-up, such as robotic devices, making most of these classical engineering approaches difficult to apply in clinical setting of rural areas due to lack of appropriate equipment.

In order to develop tools that can be easily incorporated in a routine clinical setting, we are interested in identifying the human competences to recognize and differentiate haptic stimuli during physical patient-therapist interaction. Specifically, an important endeavor is to understand the strategies and capabilities of humans to recognize between different types of hypertonic-like conditions.

In this paper we evaluated the capability of naïve subjects to discriminate between dystonic- and spastic-like arms at different level of severity by means of a physical simulator. Our results indicate that *i)* non-therapists naïve subjects may have an inherent bias to misjudge spasticity-like symptoms as dystonic and *ii)* physical manipulation characterized by high *sample entropy* (both in force and position) may lead to a misjudgment of an impairment. This is in line with Norwich's "Entropy theory of Perception" [17], which states that more accurate identification of a stimulus occurs with lower level of entropy.

Therefore, we hypothesize that specific probing motions, characterized by low *sample entropy,* but executed in appropriate directions, may facilitate the diagnosis of multi-joint hypertonia via patient-therapist physical interaction. The ultimate goal of this research is to define a set of probing motions that are characterized by low *entropy,* but that are executed in the appropriate directions so as to maximize exchange of information. This might foster the realization of simple devices that can provide immediate feedback during routine patient-therapist interaction without the need of sophisticated or expensive equipment.

D. Piovesan[†], A. Melendez-Calderon[†], and F.A. Mussa Ivaldi are with the Sensory Motor Performance Program at the Rehabilitation Institute of Chicago, Illinois, U.S.A. (e-mail: [d-piovesan, alejandro.melendez,]@northwestern.edu). *Asterisk indicates corresponding author.* [†] *indicates equal contribution*. This work was partially supported by NNINDS grant 2R01NS035673; AMC was supported by the Coolidge Postdoctoral fellowship

978-1-4673-6024-1/13/$31.00 ©2013 IEEE

II. METHODS

A. Subjects

Nine right-handed subjects (age 25 to 35 years) participated in the study. Subjects gave informed consent prior participation. Experiments were approved by the Northwestern University's Institutional Review Board.

B. Apparatus

Subjects sat in front of a two degrees of-freedom robotic manipulandum and by holding the robot's handle interacted with a series of force fields that can be proper of an impaired arm [18]. The model was implemented in Simulink and was executed in real-time using xPC Target at a rate of 1 kHz.

The subject's acromion was aligned to the imaginary line joining the robot's shoulder joint and the center of the robot's workspace. Subjects' elbow flexion and a shoulder adduction were kept approximately at 110° and 30º on the horizontal plane of the robot arm. A right arm model of patient with hypertonia (see *Neuro-mechanical model of the human arm*) was rendered as if the latter was seated facing the participants. The model's equilibrium position was such that the virtual hand matched the center of the robot's workspace. An opaque horizontal screen was interposed between the subjects' and the robot arm impeding their direct view. We projected on the screen both the image of the rendered virtual arm and a 35 cm diameter circle which was centered at the virtual arm endpoint equilibrium position. The circle was use as a representation of the virtual arm workspace. Prior of each trial, the static image of the arm was shown on the screen while a white dot indicated the position of the subject's hand and moved synchronously with it. In order to activate the trial, subjects needed to overlap the white dot to the endpoint of the virtual arm. Thus, the white dots would turn green, the virtual arm would start moving as a function of the subject hand position and the force field was rendered.

C. Experimental protocol

The experiment was divided in two successive phases: *i)* familiarization and *ii)* assessment. During *familiarization*, the participants interacted with the virtual arm where 3 conditions were presented (i.e. *normal*, *dystonic,* and *spastic*) (see Simulating hypertonic-like forces). The two impaired conditions were rendered at the maximum of their severity to clearly illustrate their salient haptic features to the subjects. Subjects' and virtual arm were connected via a virtual object (a spring-damper system) with stiffness of 1625 [N/m], critically damped. All subjects interacted sequentially with each condition in blocks of 15s for five times (5 presentations x 3 conditions = 15 trials). During this phase, a legend appeared on the top right corner of the screen indicating the condition that the subject was experiencing.

Subjects' movements were not constrained during neither during the familiarization nor during assessment. This gave us the possibility to evaluate the sample entropy of both kinetic and kinematic hand variables. During *assessment*, subjects were randomly presented with either a dystonic or spastic virtual arm where the level of severity could span between *very mild*, *mild*, *moderate* and *severe*. Subjects' task was to identify the nature of hypertonia simulated by the virtual arm. Subjects were presented each condition twelve times in blocks of 10s (2 conditions x 4 levels of severity x 14 presentations = 112 trials). The only feedback given to the subjects was the configuration of the virtual arm and the rendered force at the end effector. After the probing motion, subjects were presented with 2 yellow dots on the screen indicating a number (1,2) and the words *dystonia*, and *spasticity*. Subjects were required to select one of the two options by moving a white dot connected to the end-effector position, on top of their chosen answer.

Subjects could take as much time as they wanted to give their assessments and start a new trial. The whole experiment lasted for about 25 minutes.

TABLE I - INERTIAL AND GEOMETRICAL PARAMETERS

Symbol	Denomination	Value
$m_{subject}$	Virtual patient mass*	75 [kg]
l_1, l_2	Upper and lower arm length*	0.31,0.35 [m]
r_1, r_2	Upper and lower arm center of mass*	0.135, 0.150 [m]
m_1, m_2	Upper and lower arm mass*	2.1, 1.2 [kg]
I_1, I_2	Upper and lower arm moment of inertia about the proximal joint*	0.0593, 0.0407 [kg m^2]

D. Neuro-mechanical model of the human arm

To model the virtual arm dynamics and interaction with the environment while moving on a horizontal plane we used the following equation:

$$H(q)\ddot{q} + C(q,\dot{q})\dot{q} = J_q(q)^T \cdot F_{\text{external}} - J_\lambda{}^T \cdot \left(\Phi\left(\lambda, u(\dot{\lambda})\right) + \Psi(\lambda)\right) \quad (1)$$

$H(q)$ is the arm inertia matrix of a double pendulum system as defined in [19], q denote the vector of shoulder and elbow joint angles [rad], $C(q,\dot{q})\dot{q}$ is the term corresponding to Coriolis and centripetal forces, $J_q(q)$ is the Jacobian matrix transforming endpoint force into joint torque. Simulation-specific parameters are estimated using anthropometrical tables from Winter [20] and reported in Table I.

The Jacobian matrix J_λ [m] transforming muscle length into joint angle, was assumed to be constant [21]. This is equivalent to assume constant muscle moment arms ρ [m] at any particular position. Moment arms' values where assumed based on reported anthropometric data in the literature, so that:

$$J_\lambda(\lambda(q)) = \begin{pmatrix} -\rho_{sf} & \rho_{se} & 0 & 0 & -\rho_{bf_1} & \rho_{be_1} \\ 0 & 0 & -\rho_{ef} & \rho_{ee} & -\rho_{bf_2} & \rho_{be_2} \end{pmatrix}^T \quad (2)$$

Where the value in [m] of each moment arm is:
$\rho_{sf} = \rho_{se} = 0.03$, $\rho_{ef} = \rho_{ee} = 0.021$, $\rho_{bf_1} = \rho_{be_1} = 0.044$, $\rho_{bf_2} = \rho_{be_2} = 0.0338$ [21].

The sub-indexes correspond to *sf*, shoulder adductors (Deltoid anterior, Coracobrachialis, Pectoralis major clav.); *se,* the shoulder abductors (Deltoid posterior); *ef,* elbow flexors (Biceps long, Brachialis, Brachioradialis); *ee,* elbow extensors (Triceps lateral, Anconeus); *bf,* bi-articular flexors (Biceps short); and *be,* bi-articular extensors (Triceps long) muscle groups. The force of each muscle group is modeled as a linear combination of active (i.e. produced by a motor command *u*) and passive (i.e. produced by intrinsic rigidity of the muscles and connective tissue) components.

The force produced on each muscles' group by the motor command *u* is given by [22, 23]:

$$\Phi(\lambda, u(\dot{\lambda})) = (\varphi_{sf} \quad \varphi_{se} \quad \varphi_{ef} \quad \varphi_{ee} \quad \varphi_{bf} \quad \varphi_{be})^T$$

$$\varphi_i = \max \begin{pmatrix} 0, \\ \alpha_i u(\dot{\lambda}_i) \cdot \Gamma \cdot e^{-\left(\frac{\Gamma}{0.5u^2(\dot{\lambda}_i)+0.1}\right)^2} \end{pmatrix} \quad (3)$$

$$\Gamma = \left(\frac{\lambda_i}{\lambda_{\max,i}} - \frac{\lambda_{rest,i}}{\lambda_{\max,i}} \left(1 - u(\dot{\lambda}_i)\right) \right)$$

Where τ is the intrinsic muscle stiffness, and $u(\dot{\lambda})$ is the active motor command that is function of the muscle stretch velocity so that:

$$u(\dot{\lambda}_i) = \beta_i \min\left(1, \max\left(0, \frac{\dot{\lambda}_i}{\dot{\lambda}_{\max,i}}\right)\right) \quad | \quad \beta_i \in [0,1] \quad (4)$$

The coefficient β relates to a "stretch reflex gain". The variables $\lambda_{rest,i}$, $\lambda_{\max,i}$, and $\dot{\lambda}_{\max,i}$ are the average length of the i^{th} muscle group at rest, its maximum length and maximum rate of length change, respectively. The maximum rate of length change was computed assuming to move the end point of virtual arm along the circle of 35cm in diameter at a frequency of 2Hz.

The intrinsic rigidity of the muscles and surrounding connective tissue is function of the muscle length and generates the following force vector:

$$\Psi(\lambda) = (\psi_{sf} \quad \psi_{se} \quad \psi_{ef} \quad \psi_{ee} \quad \psi_{bf} \quad \psi_{be})^T$$

$$\psi_i = \max \begin{pmatrix} 0, \\ K_{m,i}\left(\lambda_i - \lambda_{rest,i}\right) e^{-\left(\lambda_i - \lambda_{rest,i}\right)^2} \end{pmatrix} \quad (5)$$

The term λ and K_m represent the muscle length and muscle rigidity respectively.

E. Selection of Rigidity boundary parameters

We assumed the maximum and minimum joints rigidity on literature data acquired during passive movements. [15, 24]. Based on both stroke survivors and unimpaired individuals data, we assumed that the *lower boundary* of the stiffness that we rendered as the joint passive stiffness of unimpaired individuals $K_q = \begin{pmatrix} 2 & 0.5 \\ 0.5 & 1 \end{pmatrix} [N \cdot m / rad]$. The *upper boundary* of joint rigidity was assumed to be the passive joint stiffness recorded on stroke survivors which score 4 on a Modified Ashworth Scale (MAS) $K_q = \begin{pmatrix} 14 & 3 \\ 3 & 8 \end{pmatrix} [N \cdot m / rad]$ [9, 25].

F. Simulating hypertonic-like forces

Even though hypertonia is the combination of numerous factors, our objective is to verify the participants' ability to discriminate nonlinear forces produced by abnormal position dependent stiffness (associated with dystonia) and velocity dependent stiffness (associated with spasticity). To this end, we modeled hypertonic-like forces as function of both intrinsic rigidity K_m and muscle stiffness α, as shown in eqs. (3) and (5). Our goal was to simulate a plausible scale of both dystonia and spasticity that could be recognized by our subjects via proprioceptive feedback. Haptic literature, has proposed the just noticeable difference (JND), as a parameter describing the sensitivity to biological stimuli. When the stimulus is a variation of stiffness, the JND is defined as "the ratio between the perceived difference in stiffness about a specific stiffness level and the stiffness level itself normalized to 100" (i.e. $JND = \Delta K / K \cdot 100$) [26]. Frequently, ΔK is defined as the difference between the first and the third quartile of a stiffness distribution that the subject is able to differentiate. The values of JND when testing the sensitivity of subjects to a variation of contact stiffness, strongly depend on the probing motion used to explore the environment. When a fixed displacement palpation strategy is used, the value of stiffness JND was reported to be 8% [27]. On the other hand, free exploration produces much higher values where JND was estimated to reach up to 67% [28]. Given that clinical assessments are performed with free exploration strategies we imposed a stiffness JND=60% to define the different level of dystonia. The Weber fraction of these stimuli is 0.6, defining it as the JND of the stimulus normalized to 1. Hence, we designed five intervals of adjacent stiffness levels, segmenting the rigidity range within the minimum and maximum boundary condition. The ratio between the stiffness at different levels for the specific muscle group *i* was set so that:

TABLE II - JOINT AND CARTESIAN STIFFNESS WHEN ALL MUSCLE GROUPS ARE IMPAIRED

Level of severity	υ	κ	$K_q \mid \dot{\lambda} = 0$ [N · m/rad]	$K_x \mid \dot{\lambda} = 0$ [N/m]
Normal	**0.0**	**3**	$\begin{pmatrix} 2.03 & 0.47 \\ 0.47 & 1.18 \end{pmatrix}$	$\begin{pmatrix} 23.48 & -10.65 \\ -10.65 & 17.72 \end{pmatrix}$
Very mild	**0.25**	**5**	$\begin{pmatrix} 3.39 & 0.78 \\ 0.78 & 1.96 \end{pmatrix}$	$\begin{pmatrix} 39.14 & -17.76 \\ -17.76 & 29.54 \end{pmatrix}$
Mild	**0.5**	**8**	$\begin{pmatrix} 5.43 & 1.26 \\ 1.26 & 3.15 \end{pmatrix}$	$\begin{pmatrix} 62.62 & -28.42 \\ -28.42 & 47.27 \end{pmatrix}$
Moderate	**0.75**	**13**	$\begin{pmatrix} 8.83 & 2.05 \\ 2.05 & 5.15 \end{pmatrix}$	$\begin{pmatrix} 101.76 & -46.18 \\ -46.18 & 76.82 \end{pmatrix}$
Severe	**1.0**	**21**	$\begin{pmatrix} 14.27 & 3.31 \\ 3.31 & 8.27 \end{pmatrix}$	$\begin{pmatrix} 164.39 & -74.60 \\ -74.60 & 124.10 \end{pmatrix}$

$$\frac{K_{m,i}^{level}}{K_{m,i}^{level+1}} \in \left[\frac{3}{5}, \frac{5}{8}, \frac{8}{13}, \frac{13}{21}\right] \mid level = 0..4 \Rightarrow$$
$$\Rightarrow K_{m,i}^{level} = \kappa_{\text{level}} K_{\text{nominal},i} \mid \kappa = \{3,5,8,13,21\} \quad (6)$$

We constructed the stiffness level following a Fibonacci succession that approximates a 0.6 Weber fraction. Coincidentally, our five levels of severity – *normal*, *very mild*, *mild*, *moderate* and *severe* are also similar to the five levels of MAS (i.e. 0,1,2,3,4). Indeed, at least the boundary conditions are the same where a score of 0 represents a "normal" joint stiffness and a score of 4 corresponds to our "severe" level where the joint is very hard to move. However, little can be said on the correspondence between our proposed intermediate values and the MAS scores.

It is important to observe that the Jacobian transformation is linear. Hence, multiplying the matrix of muscles' stiffness by a scalar κ will increase the joint stiffness and Cartesian stiffness by the same proportion. In order to obtain a "normal" level of rigidity with $\kappa = 3$ we imposed a nominal muscle stiffness as follows:

$$K_{\text{nominal}} = (k_{sf} \quad k_{se} \quad k_{ef} \quad k_{ee} \quad k_{bf} \quad k_{be}) = \\ (540 \quad 540 \quad 600 \quad 600 \quad 100 \quad 100) \quad [N/m] \quad (7)$$

To render the different hypertonic conditions in our experiment, the hypertonic gains (i.e. υ and ϱ in eqs. (4) and (6)) were applied to all the muscle groups and the corresponding values of joint and Cartesian stiffness are shown in Table II.

To simulate spasticity we imposed a linear variation of υ from 0 to 1 in eq. (4) so to achieve five equally spaced reflex gains levels. Literature reported ratios between K_m^{level} and α to vary between 1 and 10 [16, 29-31]. Since we assumed the intrinsic muscle stiffness α to be $K_m^{level}/4$, the variation of K_m^{level} following eq. (6) would automatically produce an increase in the active force Φ following a Weber law (see eq. (8)).

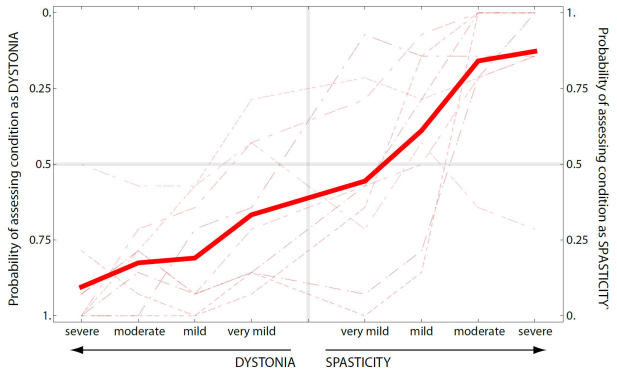

Figure 1. Mean (n=9) and individual psychometric curves showing the probability of labeling dystonia and spasticity at different levels of severities.

III. RESULTS

We constructed a psychometric curve for each subject to test the probability of assigning one specific condition. The resulting average curve highlights the low sensitivity of subject to differentiate between dystonia and spasticity (Figure 2). The curve tends to be quite flat especially when the intensity of the stimuli is low. We can observe that for the assessment of *very mild* spasticity, the probability that the subject would give a correct assessment is less than 40%. This highlights a possible intrinsic bias for subjects to select dystonia as impairment. We can also observe that the probability of misjudging spasticity at its higher level is higher compared to the same case for dystonia.

In an attempt to understand why subjects mislabeled the different conditions, we looked at the *sample entropy* (SampEn) of both the force and motion produced by the physical manipulation of the virtual arm. SampEn is an alternative metric to the approximate entropy (ApEn) [32] and it quantifies the complexity of a signal while addressing some practical problems of ApEn [33]. In a nutshell, similarly to ApEn, SampEn "quantifies the negative natural logarithm of the conditional probability (CP) that a short epoch of data, or template, is repeated during the time series. If the data are ordered, then templates that are similar for m points are often similar for m+1 points, CP approaches 1, and the negative logarithm and entropy approach 0." [33]

The calculation of SampEn requires the selection of two parameters that are: *i)* the size of the template (m), and *ii)* the tolerance for considering similar templates (r). For our analysis, we selected m=2 and r=0.2*std(trial data) as suggested by [32] for the analysis of heart rate data. For our analysis, we used the Matlab® SampEn toolbox developed by [34].

Figure 2 shows the mean force and movement SampEn calculated for each subject for both correctly and incorrectly labeled trials. We found that that force and movement

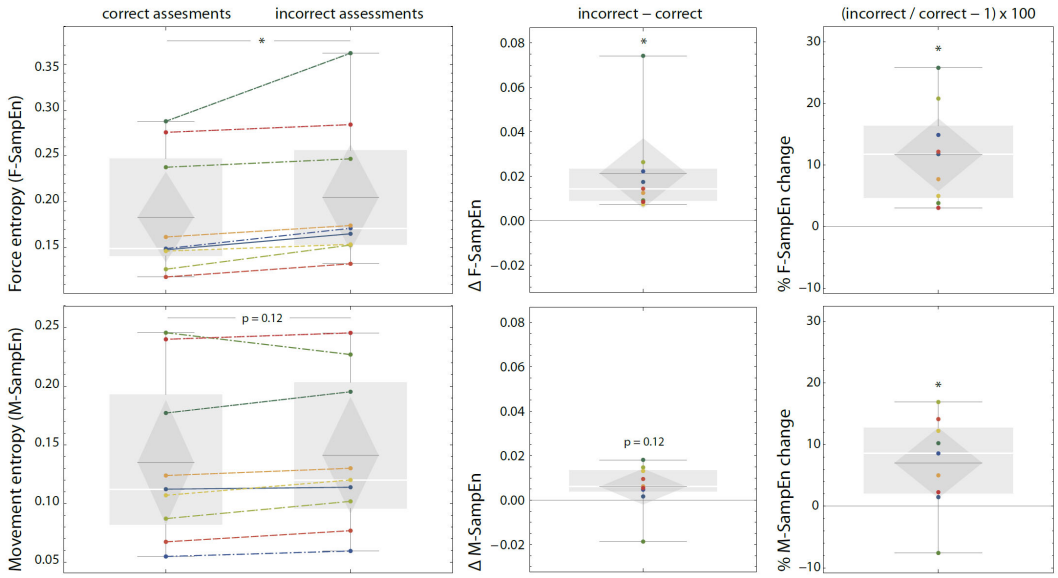

Figure 2. Calculated force and movement *sample entropy* (SampEn) of both correctly and incorrectly identified trials among subjects (n=9). Sample entropy tended to be higher during incorrectly identified trials than in those correctly assessed.

SampEn was lower in trials where a correct assessment of impairment was made. Force SampEn was more sensitive to this effect than movement SampEn. A Wilcoxon signed-rank test revealed statistical significance in force SampEn between correctly and incorrectly assessed trials ($p<0.05$), but not in movement SampEn ($p=0.12$). However, a t-test on the percentage error resulted statistically different from zero for both force and movement SampEn ($p<0.05$).

IV. Discussion

Norwich's "entropy theory of perception" defines entropy as a measure of uncertainty of the stimulus [17]. According to this theory, the value of entropy of a signal is a measure of uncertainty that directly correlates with the perception of a physical phenomenon in a leaving creature. In particular, this theory predicts that more accurate identification of a stimulus occurs with lower level of entropy. We found results that support this hypothesis by calculating the movement and force sample entropy during the interaction with impaired virtual arms and looking at the percentage of correct identification.

While several studies have been performed on the perception of force and stiffness [26], to our knowledge, our study is the first to compare the sensitivity of naive subjects to physiologically compatible stimuli within the context of multi-joint hypertonia assessment. Specifically, we tested the sensitivity of subjects to recognize dystonic- and spastic-like conditions. Our results suggest that non-therapists naïve subjects may have an inherent bias to misjudge spasticity-like symptoms as dystonic-like. While our experimental subjects could make a clear distinction between stimuli at their maximum magnitude, the individualization was difficult as the level of severity decreased. This is particularly evident for *very-mild* and *mild* impairments. It should be noted that if a submaximal setting was used to familiarize the subjects, they may have obtained a more sensitive ability to discriminate between the conditions.

While our model might not represent the whole complexity of a hypertonic arm, it can certainly capture its salient features, and it is designed following physiologically-feasible models of muscle mechanics and limb geometry. We also asked the opinion of three different licensed therapist, experts in the assessment of hypertonia; the three of them agreed that the haptic sensation produced by manipulating our model closely represented their memory of manipulating an arm at different levels of spasticity and dystonia.

The tactile sensation of mechanical stimuli during wide movement of the arm has limited influence on the overall perception [35]. The assessment of hypertonia (as in current clinical practice) relies mostly on proprioception via muscle spindles, Golgi tendon organs and skin stretch, which signals are inherently noisy [36]. Therefore, lower complexity of a stimulus may be required to better disassociation between signal and noise.

We are currently investigating *i)* the perceptual sensitivity of trained physical therapist [37], *ii)* how the perception of hypertonia is affected by the impedance introduced by the virtual connection between a patient and a clinician interacting remotely [38], and *iii)* the possibility to design specific probing motions with appropriate force sample entropy, so to increase the overall sensitivity and reduce bias.

V. Acknowledgments

We thank Prof. James Patton for his valuable suggestions.

References

[1] D. Burke, "Spasticity as an adaptation to pyramidal tract injury," *Adv Neurol,* vol. 47, pp. 401-23, 1988.

[2] J. W. Lance, "The control of muscle tone,reflexes,and movement - Wartenberg, Robert Lecture," *Neurology,* vol. 30, pp. 1303-1313, 1980.

[3] T. D. Sanger, M. R. Delgado, D. Gaebler-Spira, M. Hallett, and J. W. Mink, "Classification and definition of disorders causing hypertonia in childhood," *Pediatrics,* vol. 111, pp. e89-97, Jan 2003.

[4] B. Ashworth, "Preliminary Trial of Carisoprodol in Multiple Sclerosis," *Practitioner,* vol. 192, pp. 540 - 542, 1964.

[5] A. B. Haugh, A. D. Pandyan, and G. R. Johnson, "A systematic review of the Tardieu Scale for the measurement of spasticity," *Disability and Rehabilitation,* vol. 28, pp. 899-907, 2006/01/01 2006.

[6] R. W. Bohannon and M. B. Smith, "Interrater reliability of a modified Ashworth scale of muscle spasticity," *Phys Ther,* vol. 67, pp. 206-7, Feb 1987.

[7] A. Jethwa, J. Mink, C. Macarthur, S. Knights, T. Fehlings, and D. Fehlings, "Development of the Hypertonia Assessment Tool (HAT): a discriminative tool for hypertonia in children," *Developmental Medicine & Child Neurology,* vol. 52, pp. e83-e87, 2010.

[8] J.-O. Dyer, E. Maupas, S. de Andrade Melo, D. Bourbonnais, J. Fleury, and R. Forget, "Transmission in Heteronymous Spinal Pathways Is Modified after Stroke and Related to Motor Incoordination," *PloS one,* vol. 4, p. e4123, 2009.

[9] D. Piovesan, M. Casadio, F. A. Mussa-Ivaldi, and P. Morasso, "Comparing two computational mechanisms for explaining functional recovery in robot-therapy of stroke survivors," in *Biomedical Robotics and Biomechatronics (BioRob), 2012 4th IEEE RAS & EMBS International Conference on*, 2012, pp. 1488-1493.

[10] N. H. Mayer, A. Esquenazi, and M. K. Childers, "Common patterns of clinical motor dysfunction," *Muscle Nerve Suppl,* vol. 6, pp. S21-35, 1997.

[11] E. de Vlugt, J. de Groot, K. Schenkeveld, J. H. Arendzen, F. van der Helm, and C. Meskers, "The relation between neuromechanical parameters and Ashworth score in stroke patients," *Journal of NeuroEngineering and Rehabilitation,* vol. 7, p. 35, 2010.

[12] L. Galiana, J. Fung, and R. Kearney, "Identification of intrinsic and reflex ankle stiffness components in stroke patients," *Experimental brain research. Experimentelle Hirnforschung. Expérimentation cérébrale,* vol. 165, pp. 422-34, 2005.

[13] M. M. Mirbagheri, L. Alibiglou, M. Thajchayapong, and W. Z. Rymer, "Muscle and reflex changes with varying joint angle in hemiparetic stroke," *Journal of NeuroEngineering and Rehabilitation,* vol. 5, pp. 6-6, 2008.

[14] J. J. Palazzolo, M. Ferraro, H. I. Krebs, D. Lynch, B. T. Volpe, and N. Hogan, "Stochastic estimation of arm mechanical impedance during robotic stroke rehabilitation," *IEEE Trans Neural Syst Rehabil Eng,* vol. 15, pp. 94-103, 2007.

[15] L.-Q. Zhang, H.-S. Park, and Y. Ren, "Shoulder, elbow and wrist stiffness in passive movement and their independent control in voluntary movement post stroke," in *Rehabilitation Robotics, 2009. ICORR 2009. IEEE International Conference on*, 2009, pp. 805-811.

[16] D. Piovesan, A. Pierobon, and F. A. Mussa-Ivaldi, "Third-Order Muscle Models: The Role of Oscillatory Behavior in Force Control. ," in *International Mechanical Engineering Congress & Exposition ASME -IMECE*, Houston,TX, 2012.

[17] K. H. Norwich, "On the fundamental nature of perception," *Acta Biotheor,* vol. 39, pp. 81-90, Mar 1991.

[18] A. Melendez-Calderon*, D. Piovesan*, F. A. Mussa-Ivaldi, and J. L. Patton, "Haptic simulator of abnormal biomechanics during patient-clinician interaction," in *Proceedings of the IEEE International Conference on Robotics and Automation (ICRA) Workshop on Developments of Simulation Tools for Robotics & Biomechanics*, Karlsruhe, Germany, 2013.

[19] D. Piovesan, P. Morasso, P. Giannoni, and M. Casadio, "Arm Stiffness During Assisted Movement After Stroke: The Influence Of Visual Feedback And Training," *IEEE Transactions on Neural Systems and Rehabilitation Engineering.,* vol. 10.1109/TNSRE.2012.2226915, 2012.

[20] D. A. Winter, *Biomechanics and motor control of human movement*, 3rd ed.: John Wiley & Sons, 2004.

[21] D. W. Franklin, E. Burdet, P. T. Keng, R. Osu, C. M. Chew, T. E. Milner*, et al.*, "CNS learns stable, accurate, and efficient movements using a simple algorithm," *Journal of Neuroscience,* vol. 28, pp. 11165-11173, 2008.

[22] H. Hatze, "A myocybernetic control model of skeletal muscle," *Biological Cybernetics,* vol. 25, pp. 103-119, 1977/06/01 1977.

[23] H. Hatze, "A general myocybernetic control model of skeletal muscle," *Biological Cybernetics,* vol. 28, pp. 143-157, 1978/09/01 1978.

[24] R. L. Watts, A. W. Wiegner, and R. R. Young, "Elastic properties of muscles measured at the elbow in man: II. Patients with parkinsonian rigidity," *J Neurol Neurosurg Psychiatry,* vol. 49, pp. 1177-81, Oct 1986.

[25] J. D. Given, J. P. Dewald, and W. Z. Rymer, "Joint dependent passive stiffness in paretic and contralateral limbs of spastic patients with hemiparetic stroke," *Journal of Neurology, Neurosurgery & Psychiatry,* vol. 59, pp. 271-279, September 1, 1995 1995.

[26] W. Bing, R. L. Klatzky, and R. L. Hollis, "Force, Torque, and Stiffness: Interactions in Perceptual Discrimination," *Haptics, IEEE Transactions on,* vol. 4, pp. 221-228, 2011.

[27] H. Z. Tan, N. I. Durlach, G. L. Beauregard, and S. M.A., "Manual discrimination of compliance using active pinch grasp: The roles of force and work cues.," *Perception & Psychophysics,* vol. 57, pp. 495–510, 1995.

[28] S. Youngung and S. McMains, "Evaluation of drawing on 3D surfaces with haptics," *Computer Graphics and Applications, IEEE,* vol. 24, pp. 40-50, 2004.

[29] C. S. Cook and M. McDonagh, "Measurement of muscle and tendon stiffness in man," *european journal of applied physiology,* vol. 72, pp. 380-382, 1996.

[30] I. D. Loram, M. Lakie, I. Di Giulio, and C. N. Maganaris, "The consequences of short-range stiffness and fluctuating muscle activity for proprioception of postural joint rotations: the relevance to human standing," *Journal of Neurophysiology,* vol. 102, pp. 460-74, 2009.

[31] T. a. L. Wren, "A computational model for the adaptation of muscle and tendon length to average muscle length and minimum tendon strain," *Journal of Biomechanics,* vol. 36, pp. 1117-1124, 2003.

[32] S. M. Pincus, "Approximate entropy as a measure of system complexity," *Proceedings of the National Academy of Sciences,* vol. 88, pp. 2297-2301, March 15, 1991 1991.

[33] J. S. Richman, D. E. Lake, and J. R. Moorman, "Sample Entropy," in *Methods in Enzymology*. vol. Volume 384, L. J. Michael and B. Ludwig, Eds., ed: Academic Press, 2004, pp. 172-184.

[34] K. Lee. (2012). *Sample Entropy*. Available: http://www.mathworks.com/matlabcentral/fileexchange/35784

[35] J. J. Gibson, *The Senses Considered As Perceptual Systems*: Greenwood Press, 1966.

[36] A. A. Faisal, L. P. Selen, and D. M. Wolpert, "Noise in the nervous system," *Nat Rev Neurosci,* vol. 9, pp. 292-303, Apr 2008.

[37] A. Melendez-Calderon*, D. Piovesan*, and F. A. Mussa-Ivaldi, "Therapist discrimination of impaired muscle groups in simulated multi-joint hypertonia," in *13th Intern. Conf. on Rehab. Robotics IEEE ICORR*, 2013.

[38] D. Piovesan*, A. Melendez-Calderon*, and F. A. Mussa-Ivaldi, "Haptic perception of multi-joint hypertonia during simulated patient-therapist physical tele-interaction.," in *Conf Proc IEEE Eng Med Biol Soc.*, 2013.